IEEE Access
Multidisciplinary ⋮ Rapid Review ⋮ Open Access Journal

Received May 4, 2020, accepted June 9, 2020, date of publication June 15, 2020, date of current version June 29, 2020.

Digital Object Identifier 10.1109/ACCESS.2020.3002659

Resistive Effects on the Spatially Resolved Absolute Electroluminescence of Thin-Film Cu(In, Ga)Se_2 Solar Cells Studied by a Distributed Two-Diode Model

XIAOBO HU[1], YOUYANG WANG[1], YUN JIA[1], JIANYU HONG[1], TENGFEI CHEN[1], JUANJUAN XUE[1], YUANJING CHEN[1], JIAHUA TAO[2], GUOEN WENG[1], SHAOQIANG CHEN[1,2], ZIQIANG ZHU[1], AND JUNHAO CHU[2]

[1]Department of Electronic Engineering, East China Normal University, Shanghai 200241, China
[2]Nanophotonics and Advanced Instrument Engineering Research Center, School of Physics and Electronic Science, Ministry of Education, East China Normal University, Shanghai 200241, China

Corresponding author: Shaoqiang Chen (sqchen@ee.ecnu.edu.cn)

This work was supported in part by the National Key Research and Development Project of China under Grant 2019YFB1503402, in part by the National Natural Science Foundation of China under Grant 61604055, Grant 61704055, and Grant 61874044, in part by the Program of Shanghai Science and Technology Committee of China under Grant 17142202500, in part by the China Postdoctoral Science Foundation under Grant 2016M601543 and Grant 2018T110374, and in part by the Fundamental Research Funds for the Central Universities.

ABSTRACT Electroluminescence (EL) images with absolute photon emissions from Cu(In, Ga)Se_2 (CIGS) solar cells were obtained under different forward current injections, with the spatially distributed EL emission becoming non-uniform as the current density gradually increases. A distributed two-diode electrical three-dimensional model was established which simulated the dark current density-voltage curves and the absolute EL images of the CIGS solar cells very well. Then, the resistive effects were analyzed using this model and simulation results show that the sheet resistance of the transparent conductive oxide (TCO) layer dominates the non-uniform distribution of the EL emission in the studied CIGS thin-film solar cells. The effect of the sheet resistance of the TCO and the series resistance of the micro-diode on the EL variations is found to become obvious under high-current-injection conditions, whereas the effect of shunt resistance of the micro-diode on the EL variations becomes more obvious under low-resistance value or low-current-injection conditions.

INDEX TERMS Absolute electroluminescence, Cu(In, Ga)Se_2 thin-film solar cells, sheet resistance, distributed circuit.

I. INTRODUCTION

Electroluminescence (EL) imaging technique is powerful to characterize solar cells and modules which has gained much attention recently [1]–[13]. By measuring the spatially resolved EL emission from the top surface of solar cells, it is easy to qualitatively find failures from the EL images such as electrode faults and cell cracks which has been used in maximizing module manufacturing yields such as in crystalline silicon cells [7]–[10]. Furthermore, quantitative characterization makes it possible to extract spatially resolved information about the electronic material properties of solar cells such as minority-carrier diffusion length, diode performance, series resistance, shunts, and local junction voltage [7]–[17]. Measurements of absolute EL intensity [18] have been demonstrated usefully to obtain the internal current-voltage (I-V) relations of solar cells based on the basic reciprocity relationship [15], [16] between EL emission in light-emitting-diode (LED) operation and the external quantum efficiency (EQE) in solar-cell operation. Absolute EL imaging method has been developed to quantitative mapping the open-circuit voltage of Si solar cells and modules [19], as well as GaAs solar cells [20]–[22] and perovskite solar cells [23]. Various calibration techniques for obtaining absolute EL intensity have been proposed to characterize the properties of solar cells which demonstrated good accuracies [24].

The associate editor coordinating the review of this manuscript and approving it for publication was Diego Oliva.

It is generally known that spatial variations of electrical parameters in practical photovoltaic (PV) devices can lead to spatial inhomogeneous EL images [17]. Variations of resistance contributed from different layers of devices are significant factors to lead the non-uniform distributions in EL images [25]. Usually, it is very hard to examine the effects of different parameters experimentally since this needs large amounts of solar cell samples which is time and sample consuming. However, computer software such as the Simulation Program with Integrated Circuit Emphasis (SPICE) provides a convenient and fast technique to simulate the effects of various electrical parameters on the EL images with proper electrical models [20], [26], [27]. For current popular thin-film polycrystalline hetero-junction solar cells such as Cu(In, Ga)Se_2 (CIGS) solar cells which have inherently non-uniform electrical properties due to their granular structure, the study of the inhomogeneity issue is significant to understand the energy loss mechanism [28]. Previous works focused on studying local inhomogeneous regions such as local defects [26], [27], however, systematic works studying the influence of electrical parameters on the global absolute EL images of CIGS solar cells are few [29], [30].

In this study, a distributed two-diode electrical model established by the SPICE software was used to simulate the measured absolute EL images of a lab-sized CIGS solar cell (0.75 cm × 0.7 cm). The effects of resistive parameters such as the sheet resistance of the top transparent conductive oxide (TCO) layer, the series resistance, and the shunt resistance of the micro-diode used in the electrical model on the spatially resolved absolute EL images under different current injection conditions were systematically studied.

II. EXPERIMENTAL AND MODELING

A lab-sized CIGS solar cell with a structure of substrate (SLG)/molybdenum (Mo)/CIGS absorber/CdS/intrinsic zinc oxide (i-ZnO)/n-type aluminum doped ZnO (n-ZnO:Al)/Al grid was used in this study, in which the CIGS absorber layer was synthesized via a three-stage co-evaporation method, the details of the fabrication process and facility can be found in [31]–[37]. The total area of the cell sample is 0.75 cm × 0.7 cm, with short-circuit current density (J_{sc}) of 29.8 mA/cm^2, open-circuit voltage (V_{oc}) of 0.683 V, fill factor of 0.495, and energy conversion efficiency (η) of 10.1% measured under AM1.5G, 1-sun illumination condition using a solar simulator at room temperature. Absolute EL images of the CIGS solar cell were obtained using radiant-flux LED standards for calibration [18]. Planar LEDs with a circular aperture were prepared, the total absolute radiant fluxes of which were calibrated and used as radiant-flux standards in the measurements, the detailed structures of the planar LEDs and experimental procedures were presented elsewhere [18].

A two-diode electrical model that approximately describes the cell topology was used in order to conduct the spatial simulation in SPICE. The part of the model is shown in Fig. 1 which consists of four layers. The top layer is a grid contact layer representing the electrode metal layer (aluminum, Al), with a distributed resistor denoted by R_m, similar descriptions are used for other layers. The layer under the grid contact is a resistive grid layer (R_{TCO}) representing the TCO layer (n-ZnO:Al in our cell sample). The bottom layer is also a grid (R_b) representing the back contact (Mo here). Between the TCO layer and the bottom layer, there is an active layer composing of micro-diodes. Each micro-diode is represented with a modified two-diode model of the solar cell representing the CdS-CIGS heterojunction structure and the CIGS bulk resistance (r_s-series resistance; r_{sh}-shunt resistance; n_1, n_2-ideality factors; j_{01}, j_{02}-saturation current densities). The negative probe is connected to the distributed resistors representing the Al electrode layer contact with the TCO and placed above the TCO layer in the top layer. The positive probe is connected to the bottom layer in the center of the cell. Thus, the simulated contacting scheme replicates that of the EL measurements. The main parameters describing the two-diode model of micro-diode in the dark are shown in Fig. 1, with one diode describing diffusion current (j_{01}) and the other one describing recombination current (j_{02}) [38].

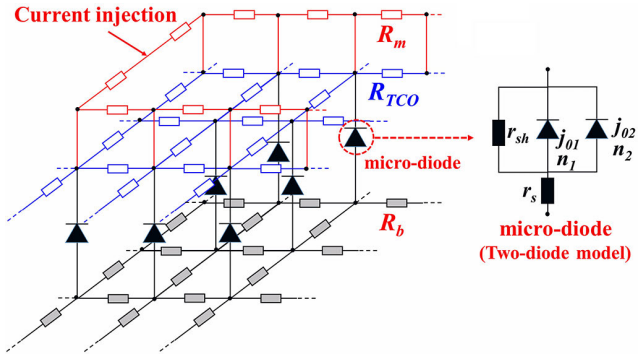

FIGURE 1. Part of the distributed two-diode electrical model of CIGS solar cell for EL simulations by SPICE. R_m: distributed resistor of the top electrode metal layer; R_{TCO}: distributed resistor of the TCO layer; R_b: distributed resistor of the bottom contact layer; Each micro-diode is represented with a modified two-diode current model, r_s-series resistance; r_{sh}-shunt resistance; n_1, n_2- ideality factors; j_{01}, j_{02}-saturation current densities.

The parameters of the micro-diode were extracted from the dark current density-voltage (J-V) characteristic of the cell: where N is the total number of micro-diodes according to the meshing of the cell's active area. $N = 900$ was selected in this work considering both the time consumption and smoothness of the simulations. Initial values of the parameters used for SPICE simulation were calculated by multiplication of cell resistances (R_s and R_{sh}) with the number of micro-diodes (N) since the micro-diodes are connected in parallel both micro-diode resistances (r_s and r_{sh}). Due to the square grid used for simulations, the values of R_{TCO} and R_b were numerically identical to sheet resistances R_{TCO} and R_b [6]. The initial values of R_{TCO}, R_b, and R_m were referred from literature [6]. Then an iterative procedure was implemented until the fitting results approximate experimental results, the deviation was controlled smaller than 1%.

In practice, the main parameters that influence the simulated CIGS cell's J-V curve, as well as the EL distribution throughout the cell, are series resistance r_s, shunt resistance r_{sh}, and TCO resistance R_{TCO}, whereas R_b and R_m are usually too small and negligible [6]. To determine the correct values of these parameters, SPICE simulations of the dark J-V and EL emission were iteratively performed. When both simulations adequately fitted the measurements, the values of parameters were determined.

III. RESULTS AND DISCUSSION

Absolute EL images obtained with different injection current densities from 5 mA/cm^2 to 50 mA/cm^2 are shown in Fig. 2, note that the dark edges of the images are the background. It can be seen that as current density increases, the absolute EL intensity increases and the EL emission distribution becomes more inhomogeneous and high intensity of EL emission concentrates around the grid Al electrode. The EL emission intensity is symmetrical with respect to the top Al grid, indicating the relevent resistances are uniformly distribited.

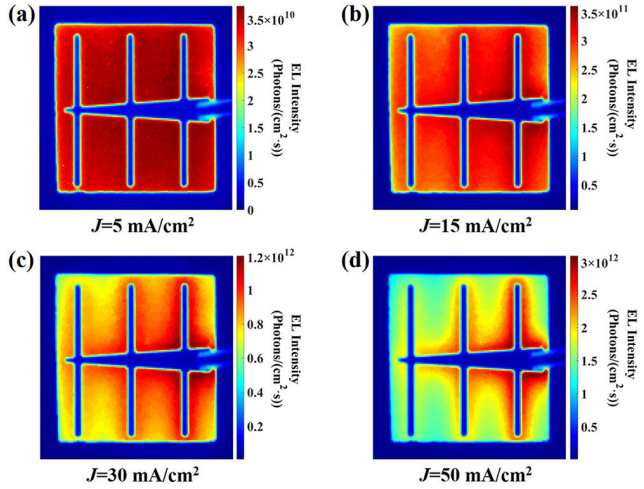

FIGURE 2. EL images (absolute photon emission rate) of a CIGS solar cell with 10.1% efficiency as a function of different injection current density from 5 to 50 mA/cm^2 by using radiant-flux LED standards for calibration [24].

Fig. 3 shows the result of the simulation, a dark J–V characteristic is directly compared with the measured J–V characteristic. Dark J–V simulation was performed as a direct-current (DC) sweep analysis of a voltage source connected to the provided nodes. A two-diode model was used to describe the J-V characteristics of the micro-diode by using the following equation,

$$j = j_{01}\exp\left(\frac{q\,(V - j\cdot r_s)}{n_1 kT}\right) + j_{02}\exp\left(\frac{q\,(V - j\cdot r_s)}{n_2 kT}\right) + \frac{V - j\cdot r_s}{r_{sh}} \quad (1)$$

where j is the total current density of one unit of the two-diode, q is the elementary charge, k is the Boltzmann

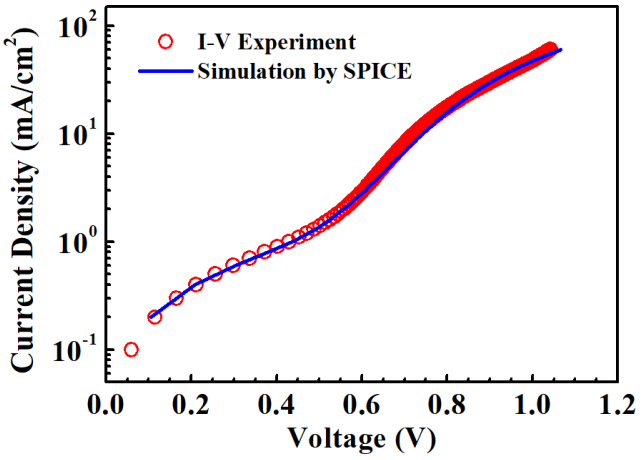

FIGURE 3. I-V relationship from I-V experiment (circle symbol) and simulation (solid line) by SPICE using two-diode electrical model.

constant, and T is the Kelvin temperature, the other parameters have been defined in previous content. Note that the r_s is fine-tuned when transforming to the model parameter, since the r_s in Eq. (1) also contains R_{TCO}, R_m, and R_b. By using this model, good fitting results can be obtained as Fig. 3 shows.

Under forward injection current, the local voltage bias on each micro-diode unit could be extracted using the SPICE simulation and the absolute EL emission rate could be obtained according to the reciprocity relationship as following shows [15],

$$\phi_{emi}(E) = Q_{ei}(E)\phi_{bb}(E)\exp(qV_i/kT) \quad (2)$$

where $Q_{ei}(E)$ is the EQE of the solar cell, E is the photon energy, V_i is the local junction voltage on the ith micro-diode, and φ_{bb} is the spectral flux density of a black body, which depends on Planck's constant h and the vacuum speed c of light, given by Equation (3),

$$\phi_{bb}(E) = \frac{2\pi E^2}{h^3c^2}\exp(-E/kT) \quad (3)$$

Then, the injection current density-dependent absolute EL emission intensities of the total micro-diodes were obtained and compared to the measured absolute EL emission, as well as the external EL quantum yield (y_{ext}^{LED}, defined as the ratio of average absolute EL emission rate over the injected electrons per unit area [18]) dependent on injection current density under the operation of an LED, and the results are shown in Fig. 4. It can be found that there is still a small difference between the simulated and experimental in EL emissions and y_{ext}^{LED} dependent on injection current. This reason for the difference may due to the actually existed spatially inhomogeneous properties for real solar cells, that is, the poorer diode quality factors may be different for each micro-region on the sample, whereas the model used for simulation is spatially uniform. The fitted power-law relation [6] ($I_{EL} \sim J^b$, I_{EL}: EL intensity, J: current density, b: power law exponent) of the absolute EL emission dependent on current density are

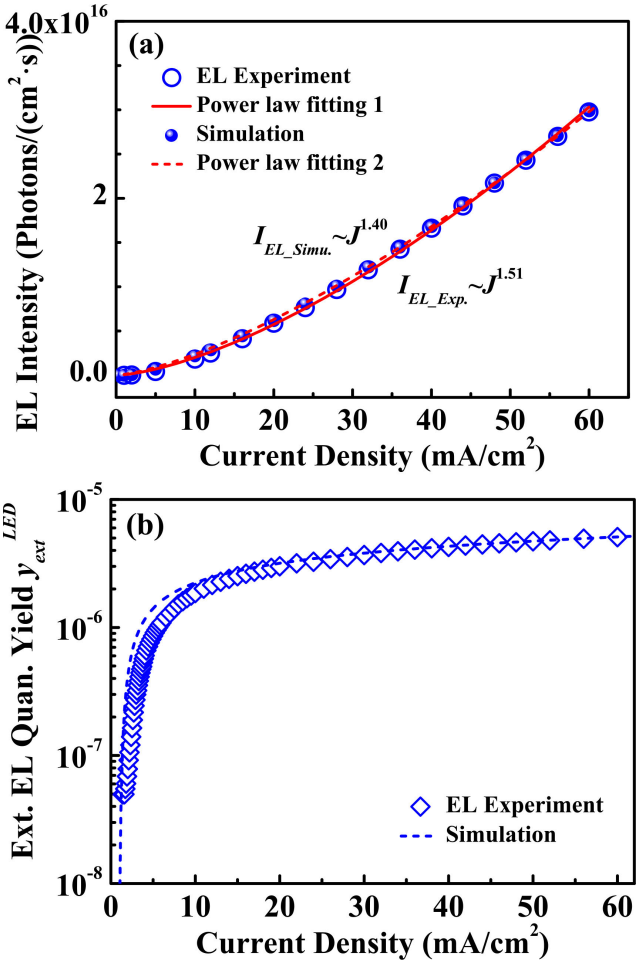

FIGURE 4. Current density dependence of (a) the absolute EL intensity, which is the sum of the absolute values for the total pixels in the measured absolute EL images (the two lines show the fitting results using power-law relation), (b) the external EL quantum yield (Ext. EL. Quan. Yield) of the sample under the operation of an LED (y_{ext}^{LED}).

also shown for both experimental and simulation results in Fig. 4 (a). The power-law exponent of the simulation EL is smaller than that of the experimental results [6]. This empirical exponent can actually be viewed as the diode quality factor of the one-diode model [15], [39]. Please note that, despite the one-diode model can fit the injection dependence of the EL intensity quite well, the two-diode model was reported to be more decent for simulating both electrical and luminescence properties of the studied samples [40]. Thus, the larger exponent obtained from the experimental result than the simulated result may also be attributed to the inhomogeneous characteristics of real solar cells with poorer diode quality factors.

Fig. 5(a) shows an example of the simulation results of the absolute EL emission image from the CIGS solar cell with a forward injection current density of 30 mA/cm^2. Note that the darker edges around the simulated image are attributed to the degraded EL intensity at the edge of the solar cell sample. This image approximates to the real EL image in Fig. 5(b)

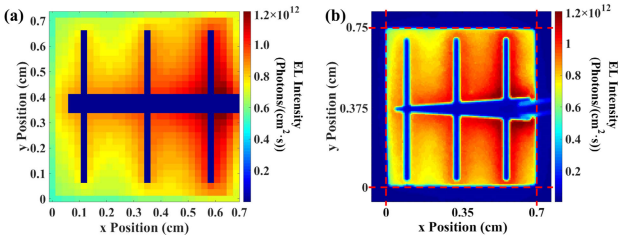

FIGURE 5. (a) Simulated and (b) measured absolute EL image with an injection current density of 30 mA/cm^2.

with an injection current density of 30 mA/cm^2, while the concentration of the EL emission around the grid Al electrode can also be observed clearly.

Fig. 6 shows the comparison of the normalized EL profiles from experimental absolute EL measurements and absolute EL emission simulations in two directions, which are in parallel to (x-direction) and vertical to (y-direction) the main

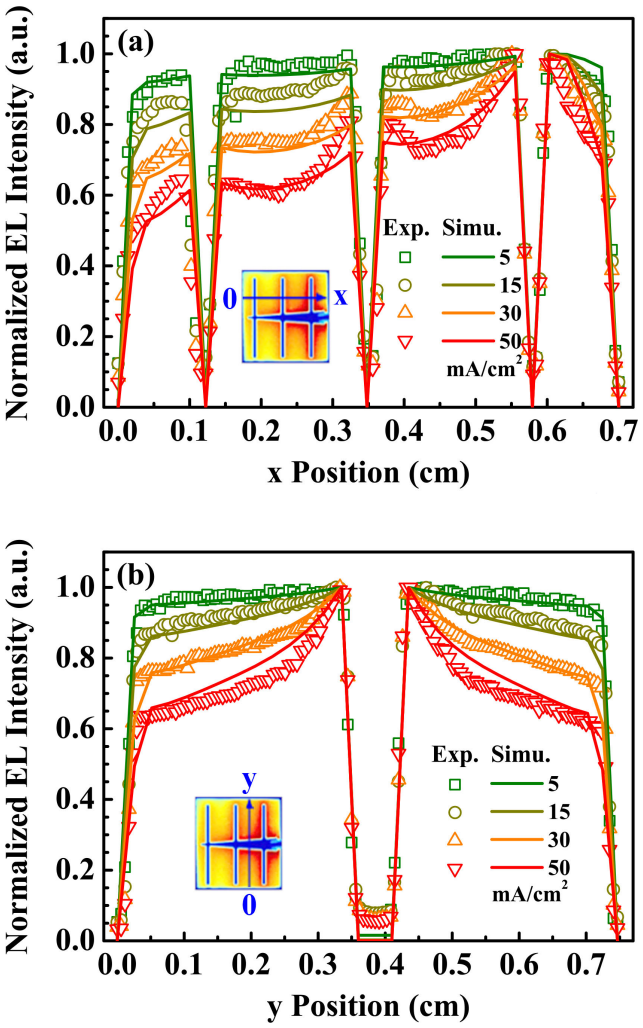

FIGURE 6. Normalized EL profiles from experimental absolute EL measurements and absolute EL emission simulations in (a) x-direction and (b) y-direction.

grid electrodes in the plane of the solar cell's surface. It can be seen that in *y*-direction, the simulation results are well-fitted the experimental results for all injection currents by using the fitting parameters listed in Table 1, this indicates that along *y*-direction, the properties of the solar cell are uniform. In *x*-direction, however, divergence can be found between the experimental and simulated results, especially in the two outer sides of the cell, this indicates that along *x*-direction, the solar cell still shows inhomogeneity properties even if the dark edges were considered in our simulations. The similar phenomenon can also be demonstrated in some types of solar cells, such as monocrystalline Si and GaAs [20], [41]. However, for other types of materials like multi-crystalline Si, the resistive effects show strong lateral inhomogeneities in the whole spatial distribution, and the values of the relevant resistances are found to be larger away from the busbar or near the cracks, which may require to utilize some 2-D finite element simulation methods [42]–[50].

TABLE 1. Parameters used in the simulation.

Resistor	r_s ($\Omega\cdot cm^2$)	r_{sh} ($\Omega\cdot cm^2$)	R_{TCO} ($\Omega\cdot\square$)	R_m ($\Omega\cdot\square$)	R_b ($\Omega\cdot\square$)
Value	0.3	520	22	0.2	0.2
j* and *n	j_{01} (mA/cm^2)	n_1	j_{02} (mA/cm^2)	n_2	
Value	1.0×10^{-9}	1.51	4.1×10^{-4}	2.72	

Based on the resistive parameters in Table 1, we tried to simulate and investigate the effect of resistive parameters on the inhomogeneity properties of the solar cells, since it is hard to really prepare CIGS solar cells with desired parameters whereas simulation supplies a convenient way. The investigation method was to change one parameter while keeping the other ones unvaried. Fig. 7 shows the absolute EL emission profiles dependent on the sheet resistance of the TCO layer (R_{TCO}) in the two directions as shown in the two insets of the respective figure, with injection current density of 30 mA/cm^2. It can be seen that the non-uniformity of the EL profile becomes more severe as the TCO sheet resistance increases. From center to outer along *y*-direction as shown in Fig. 7 (b), the absolute EL intensity is firstly higher with larger R_{TCO}, but the decreasing of the intensity is also faster for larger R_{TCO}, so after some point along *y*-direction, the absolute EL intensity gets lower for larger R_{TCO}. However, the distance between two sub-grids is too close to observe the same phenomenon of crossing along *x*-direction, as shown in Fig. 7 (a).

Fig. 8 (a) and (b) show the influence of the series resistance r_s on the absolute EL emission profiles in *y*-direction under high (30 mA/cm^2) and low (1 mA/cm^2)-current-injection conditions, respectively. In high-current-injection conditions, all the EL emission profiles show non-uniformity properties. Besides, as r_s increases, the EL emission profiles become more homogeneous, this effect is opposite to that of R_{TCO} as shown in Fig. 7. In low-current-injection conditions, it gets

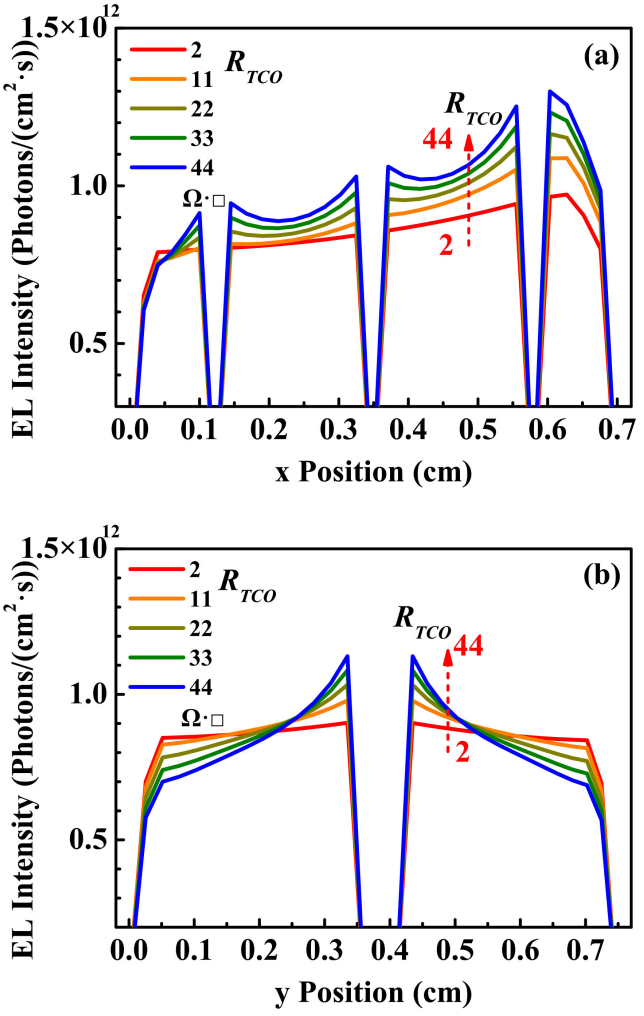

FIGURE 7. Influence of R_{TCO} on the EL emission profiles in (a) *x*-direction and (b) *y*-direction.

hard to distinguish the EL emission profiles with different r_s since all the profiles become almost uniform in this direction. Fig. 8 (c) and (d) show the influence of the shunt resistance r_{sh} on the absolute EL emission profiles in *y*-direction under the two current injection conditions. Note that the variation of the global r_{sh} in each micro diode can be caused by the instability of the cell fabrication processes. In high-current-injection conditions, all the EL emission profiles show inhomogeneous and parallel characteristics along *y*-direction, and it is hard to distinguish the absolute EL emission profiles with the r_{sh} increased from initial 520 to 720 $\Omega\cdot cm^2$, whereas the degradation of EL emission starts to be obvious as the r_{sh} decreased from 520 to 320 $\Omega\cdot cm^2$, indicate that too low shunt resistance will increase the leakage current in the solar cell and seriously affect the EL emission. In low-current-injection conditions, all the EL emission profiles become almost uniform, and it is very easy to distinguish the EL emission profiles with different r_{sh}, as the absolute EL intensity increases rapidly with increased r_{sh}. It should be noted although this work studies the influence of electrical parameters on the global absolute EL images, the results are also useful for determining the type

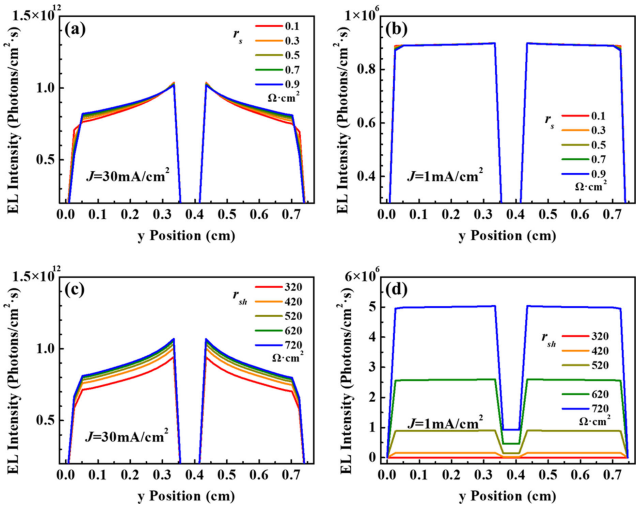

FIGURE 8. Influence of (a) (b) series resistance r_S and (c) (d) shunt resistance r_{sh} on the EL variations in y-direction under high (30 mA/cm^2) and low (1 mA/cm^2)-current-injection conditions, respectively.

of local resistive singularity induced defects by analyzing local inhomogeneity in EL images under different injection conditions.

IV. CONCLUSION

Spatially resolved EL images with absolute emissions for CIGS solar cells measured under different forward current injection conditions were well simulated by SPICE using a two-diode electrical model. By fitting the simulated dark J-V curve and the absolute EL images with the experimental results, resistive parameters such as R_{TCO}, r_s, and r_{sh} were extracted. Further simulations have shown that the R_{TCO} dominated the non-uniform distribution of the absolute EL emission around the electrode contacts in the CIGS thin-film solar cells. Simulations also show that the influence of the R_{TCO} and the r_s on the absolute EL emission profiles are obvious under high-current-injection conditions, whereas the influence of the r_{sh} on the absolute EL emission profiles become more obvious under low-resistance-value or low-current-injection conditions.

ACKNOWLEDGMENT

The authors thank Dr. Jingwei Chen, College of Physics Science and Technology, Institute of Photovoltaics, Hebei University, Baoding, China, for providing the solar cell samples. This work was supported by the Research Funds of MoE Nanophotonics and Advanced Instrument Engineering Research Center and the Fundamental Research Funds for the Central Universities. *(Xiaobo Hu and Youyang Wang are co-first authors.)*

REFERENCES

[1] T. Fuyuki, H. Kondo, T. Yamazaki, Y. Takahashi, and Y. Uraoka, "Photographic surveying of minority carrier diffusion length in polycrystalline silicon solar cells by electroluminescence," *Appl. Phys. Lett.*, vol. 86, no. 26, pp. 1–3, 2005, doi: 10.1063/1.1978979.

[2] F. Fruehauf and M. Turek, "Quantification of electroluminescence measurements on modules," *Energy Procedia*, vol. 77, pp. 63–68, Aug. 2015, doi: 10.1016/j.egypro.2015.07.010.

[3] G. W. Shu, J. Y. Lin, H. T. Jian, J. L. Shen, S. C. Wang, C. L. Chou, W. C. Chou, C. H. Wu, C. H. Chiu, and H. C. Kuo, "Optical coupling from InGaAs subcell to InGaP subcell in InGaP/InGaAs/Ge multi-junction solar cells," *Opt. Express*, vol. 21, no. S1, p. A123, Jan. 2013, doi: 10.1364/oe.21.00a123.

[4] M. Seeland, R. Rösch, and H. Hoppe, "Quantitative analysis of electroluminescence images from polymer solar cells," *J. Appl. Phys.*, vol. 111, no. 2, Jan. 2012, Art. no. 024505, doi: 10.1063/1.3677981.

[5] Z. Hameiri, A. M. Soufiani, M. K. Juhl, L. Jiang, F. Huang, Y.-B. Cheng, H. Kampwerth, J. W. Weber, M. A. Green, and T. Trupke, "Photoluminescence and electroluminescence imaging of perovskite solar cells," *Prog. Photovolt., Res. Appl.*, vol. 23, no. 12, pp. 1697–1705, Dec. 2015, doi: 10.1002/pip.2716.

[6] M. Bokalič, J. Raguse, J. R. Sites, and M. Topič, "Analysis of electroluminescence images in small-area circular CdTe solar cells," *J. Appl. Phys.*, vol. 114, no. 12, Sep. 2013, Art. no. 123102, doi: 10.1063/1.4820392.

[7] B. Li, A. Stokes, and D. M. J. Doble, "Evaluation of two-dimensional electrical properties of photovoltaic modules using bias-dependent electroluminescence," *Prog. Photovolt., Res. Appl.*, vol. 20, no. 8, pp. 936–944, Dec. 2012, doi: 10.1002/pip.1161.

[8] P. Chaturvedi, B. Hoex, and T. M. Walsh, "Broken metal fingers in silicon wafer solar cells and PV modules," *Sol. Energy Mater. Sol. Cells*, vol. 108, pp. 78–81, Jan. 2013, doi: 10.1016/j.solmat.2012.09.013.

[9] A. Kitiyanan, A. Ogane, A. Tani, T. Hatayama, H. Yano, Y. Uraoka, and T. Fuyuki, "Comprehensive study of electroluminescence in multicrystalline silicon solar cells," *J. Appl. Phys.*, vol. 106, no. 4, pp. 1–5, 2009, doi: 10.1063/1.3204942.

[10] M. Schneemann, T. Kirchartz, R. Carius, and U. Rau, "Measurement and modeling of reverse biased electroluminescence in multi-crystalline silicon solar cells," *J. Appl. Phys.*, vol. 114, no. 13, Oct. 2013, Art. no. 134509, doi: 10.1063/1.4824099.

[11] H. Nesswetter, W. Dyck, P. Lugli, A. W. Bett, and C. G. Zimmermann, "Luminescence based series resistance mapping of III-V multijunction solar cells," *J. Appl. Phys.*, vol. 114, no. 19, Nov. 2013, Art. no. 194510, doi: 10.1063/1.4831749.

[12] M. Seeland, C. Kästner, and H. Hoppe, "Quantitative evaluation of inhomogeneous device operation in thin film solar cells by luminescence imaging," *Appl. Phys. Lett.*, vol. 107, no. 7, Aug. 2015, Art. no. 073302, doi: 10.1063/1.4929343.

[13] K. Ramspeck, K. Bothe, D. Hinken, B. Fischer, J. Schmidt, and R. Brendel, "Recombination current and series resistance imaging of solar cells by combined luminescence and lock-in thermography," *Appl. Phys. Lett.*, vol. 90, no. 15, pp. 10–13, 2007, doi: 10.1063/1.2721138.

[14] P. Würfel, T. Trupke, T. Puzzer, E. Schäffer, W. Warta, and S. W. Glunz, "Diffusion lengths of silicon solar cells from luminescence images," *J. Appl. Phys.*, vol. 101, no. 12, Jun. 2007, Art. no. 123110, doi: 10.1063/1.2749201.

[15] U. Rau, "Reciprocity relation between photovoltaic quantum efficiency and electroluminescent emission of solar cells," *Phys. Rev. B, Condens. Matter*, vol. 76, no. 8, pp. 1–8, Aug. 2007, doi: 10.1103/PhysRevB.76.085303.

[16] T. Kirchartz, A. Helbig, W. Reetz, M. Reuter, J. H. Werner, and U. Rau, "Reciprocity between electroluminescence and quantum efficiency used for the characterization of silicon solar cells," *Prog. Photovolt., Res. Appl.*, vol. 17, no. 6, pp. 394–402, Sep. 2009, doi: 10.1002/pip.895.

[17] D. Hinken, K. Ramspeck, K. Bothe, B. Fischer, and R. Brendel, "Series resistance imaging of solar cells by voltage dependent electroluminescence," *Appl. Phys. Lett.*, vol. 91, no. 18, pp. 10–13, 2007, doi: 10.1063/1.2804562.

[18] S. Chen, L. Zhu, M. Yoshita, T. Mochizuki, C. Kim, H. Akiyama, M. Imaizumi, and Y. Kanemitsu, "Thorough subcells diagnosis in a multijunction solar cell via absolute electroluminescence-efficiency measurements," *Sci. Rep.*, vol. 5, no. 1, pp. 1–6, Jul. 2015, doi: 10.1038/srep07836.

[19] T. Mochizuki, C. Kim, M. Yoshita, J. Mitchell, Z. Lin, S. Chen, H. Takato, Y. Kanemitsu, and H. Akiyama, "Solar-cell radiance standard for absolute electroluminescence measurements and open-circuit voltage mapping of silicon solar modules," *J. Appl. Phys.*, vol. 119, no. 3, Jan. 2016, Art. no. 034501, doi: 10.1063/1.4940159.

[20] X. Hu, T. Chen, J. Hong, S. Chen, G. Weng, Z. Zhu, and J. Chu, "Diagnosis of GaAs solar-cell resistance via absolute electroluminescence imaging and distributed circuit modeling," *Energy*, vol. 174, pp. 85–90, May 2019, doi: 10.1016/j.energy.2019.02.170.

[21] X. Hu, L. Zhu, G. Weng, and S. Chen, "Accessing externally induced spatially-resolved strain in GaAs thin-film solar cells by electroluminescence imaging," *Sol. Energy Mater. Sol. Cells*, vol. 179, pp. 283–288, Jun. 2018, doi: 10.1016/j.solmat.2017.12.019.

[22] X. Hu, T. Chen, J. Xue, G. Weng, S. Chen, H. Akiyama, and Z. Zhu, "Absolute electroluminescence imaging diagnosis of GaAs thin-film solar cells," *IEEE Photon. J.*, vol. 9, no. 5, pp. 1–9, Oct. 2017, doi: 10.1109/JPHOT.2017.2731800.

[23] J. Xue, X. Hu, Y. Guo, G. Weng, J. Jiang, S. Chen, Z. Zhu, J. Chu, and H. Akiyama, "Diagnosis of perovskite solar cells through absolute electroluminescence-efficiency measurements," *Frontiers Phys.*, vol. 7, pp. 1–7, Oct. 2019, doi: 10.3389/fphy.2019.00166.

[24] M. Yoshita, L. Zhu, C. Kim, T. Mochizuki, T. Nakamura, M. Imaizumi, S. Chen, H. Kubota, Y. Kanemitsu, and H. Akiyama, "Calibration standards and measurement accuracy of absolute electroluminescence and internal properties in multi-junction and arrayed solar cells," *Proc. SPIE*, vol. 9743, Mar. 2016, Art. no. 97430D, doi: 10.1117/12.2211726.

[25] J. Haunschild, M. Glatthaar, M. Kasemann, S. Rein, and E. R. Weber, "Fast series resistance imaging for silicon solar cells using electroluminescence," *Phys. Status Solidi (RRL)-Rapid Res. Lett.*, vol. 3, nos. 7–8, pp. 227–229, Oct. 2009, doi: 10.1002/pssr.200903175.

[26] K. Brecl and M. Topič, "Simulation of losses in thin-film silicon modules for different configurations and front contacts," *Prog. Photovolt., Res. Appl.*, vol. 16, no. 6, pp. 479–488, Sep. 2008, doi: 10.1002/pip.831.

[27] P. Sharma, M. Wilkins, H. Schriemer, and K. Hinzer, "Modeling nonuniform irradiance and chromatic aberration effects in a four junction solar cell using SPICE," in *Proc. IEEE 40th Photovolt. Spec. Conf. (PVSC)*, Jun. 2014, pp. 3293–3297, doi: 10.1109/PVSC.2014.6925639.

[28] S. Johnston, T. Unold, I. Repins, A. Kanevce, K. Zaunbrecher, F. Yan, J. V. Li, P. C. Dippo, R. Sundaramoorthy, K. M. Jones, and B. To, "Correlations of Cu(In, Ga)Se_2 imaging with device performance, defects, and microstructural properties," *J. Vac. Sci. Technol. A, Vac. Surf. Films*, vol. 30, no. 4, 2012, Art. no. 04D111, doi: 10.1116/1.4714358.

[29] U. Rau and J. H. Werner, "Radiative efficiency limits of solar cells with lateral band-gap fluctuations," *Appl. Phys. Lett.*, vol. 84, no. 19, pp. 3735–3737, May 2004, doi: 10.1063/1.1737071.

[30] A. Helbig, T. Kirchartz, R. Schaeffler, J. H. Werner, and U. Rau, "Quantitative electroluminescence analysis of resistive losses in Cu(In, Ga)Se_2 thin-film modules," *Sol. Energy Mater. Sol. Cells*, vol. 94, no. 6, pp. 979–984, Jun. 2010, doi: 10.1016/j.solmat.2010.01.028.

[31] W. Zhang, H. Zhu, L. Zhang, Y. Guo, X. Niu, Z. Li, J. Chen, Q. Liu, and Y. Mai, "Cu(In, Ga)Se_2 thin film solar cells grown at low temperatures," *Solid-State Electron.*, vol. 132, pp. 57–63, Jun. 2017, doi: 10.1016/j.sse.2017.03.003.

[32] H. Li, F. Qu, H. Luo, X. Niu, J. Chen, Y. Zhang, H. Yao, X. Jia, H. Gu, and W. Wang, "Engineering CIGS grains qualities to achieve high efficiency in ultrathin Cu(In_xGa_{1-x})Se_2 solar cells with a single-gradient band gap profile," *Results Phys.*, vol. 12, pp. 704–711, Mar. 2019, doi: 10.1016/j.rinp.2018.12.043.

[33] X. Niu, H. Zhu, W. Zhang, X. Laing, Y. Guo, Z. Li, J. Chen, Y. Xu, and Y. Mai, "Control of oxygen for magnetron sputtered ZnO:Al window layer in Cu(In,Ga)Se_2 thin film solar cells," *Phys. Status Solidi A*, vol. 214, no. 10, Oct. 2017, Art. no. 1700132, doi: 10.1002/pssa.201700132.

[34] C. Zhang, H. Zhu, X. Liang, D. Zhou, Y. Guo, X. Niu, Z. Li, J. Chen, and Y. Mai, "Influence of heating temperature of se effusion cell on Cu(In, Ga)Se_2 thin films and solar cells," *Vacuum*, vol. 141, pp. 89–96, Jul. 2017, doi: 10.1016/j.vacuum.2017.03.027.

[35] Y. Guo, H. Zhu, X. Niu, W. Zhang, Z. Li, J. Chen, and Y. Mai, "Influence of substrate temperature on LPCVD ZnO thin film and Cu(In, Ga)Se_2 thin film solar cells," *Adv. Eng. Mater.*, vol. 18, no. 8, pp. 1418–1425, Aug. 2016, doi: 10.1002/adem.201600113.

[36] X. Liang, H. Zhu, J. Chen, D. Zhou, C. Zhang, Y. Guo, X. Niu, Z. Li, and Y. Mai, "Substrate temperature optimization for Cu(In, Ga)Se_2 solar cells on flexible stainless steels," *Appl. Surf. Sci.*, vol. 368, pp. 464–469, Apr. 2016, doi: 10.1016/j.apsusc.2016.02.003.

[37] D. Zhou, H. Zhu, X. Liang, C. Zhang, Z. Li, Y. Xu, J. Chen, L. Zhang, and Y. Mai, "Sputtered molybdenum thin films and the application in CIGS solar cells," *Appl. Surf. Sci.*, vol. 362, pp. 202–209, Jan. 2016, doi: 10.1016/j.apsusc.2015.11.235.

[38] O. Breitenstein and S. Rißland, "A two-diode model regarding the distributed series resistance," *Sol. Energy Mater. Sol. Cells*, vol. 110, pp. 77–86, Mar. 2013, doi: 10.1016/j.solmat.2012.11.021.

[39] K. J. Price, A. Vasko, L. Gorrelland, and A. D. Compaan, "Temperature-dependent electroluminescence from CdTe/CdS solar cells," in *Proc. Mater. Res. Soc. Symp.*, vol. 763, 2003, pp. 195–200, doi: 10.1557/proc-763-b5.9.

[40] T. Fuyuki and A. Kitiyanan, "Photographic diagnosis of crystalline silicon solar cells utilizing electroluminescence," *Appl. Phys. A, Mater. Sci. Process.*, vol. 96, no. 1, pp. 189–196, 2009, doi: 10.1007/s00339-008-4986-0.

[41] J. Hong, Y. Wang, Y. Chen, X. Hu, G. Weng, S. Chen, H. Akiyama, Y. Zhang, B. Zhang, and J. Chu, "Absolute electroluminescence imaging with distributed circuit modeling: Excellent for solar-cell defect diagnosis," *Prog. Photovolt., Res. Appl.*, vol. 28, no. 4, pp. 295–306, Apr. 2020, doi: 10.1002/pip.3236.

[42] F. Frühauf and O. Breitenstein, "Improved Laplacian photoluminescence image evaluation regarding the local diode back voltage distribution," *Sol. Energy Mater. Sol. Cells*, vol. 174, pp. 277–282, Jan. 2018, doi: 10.1016/j.solmat.2017.09.001.

[43] F. Frühauf, J. Wong, J. Bauer, and O. Breitenstein, "Finite element simulation of inhomogeneous solar cells based on lock-in thermography and luminescence imaging," *Sol. Energy Mater. Sol. Cells*, vol. 162, pp. 103–113, Apr. 2017, doi: 10.1016/j.solmat.2016.12.037.

[44] F. Frühauf, J. Wong, and O. Breitenstein, "Luminescence based high resolution finite element simulation of inhomogeneous solar cells," *Sol. Energy Mater. Sol. Cells*, vol. 189, pp. 133–137, Jan. 2019, doi: 10.1016/j.solmat.2018.09.030.

[45] O. Breitenstein, F. Frühauf, and J. Bauer, "Advanced local characterization of silicon solar cells," *Phys. Status Solidi Appl. Mater. Sci.*, vol. 214, no. 12, pp. 1–12, 2017, doi: 10.1002/pssa.201700611.

[46] J. M. Wagner, K. Upadhyayula, J. Carstensen, and R. Adelung, "Averaging the unaverageable: Defining a meaningful local series resistance for large-area silicon solar cells," *AIP Conf.*, vol. 2147, Aug. 2019, Art. no. 020019, doi: 10.1063/1.5123824.

[47] F. Frühauf, Y. Sayad, and O. Breitenstein, "Description of the local series resistance of real solar cells by separate horizontal and vertical components," *Sol. Energy Mater. Sol. Cells*, vol. 154, pp. 23–34, Sep. 2016, doi: 10.1016/j.solmat.2016.04.010.

[48] O. Breitenstein, J. Bauer, T. Trupke, and R. A. Bardos, "On the detection of shunts in silicon solar cells by photo- and electroluminescence imaging," *Prog. Photovolt., Res. Appl.*, vol. 16, no. 4, pp. 325–330, Jun. 2008, doi: 10.1002/pip.803.

[49] T. M. Pletzer, J. I. van Molken, S. Rissland, B. Hallam, E. Cornagliotti, J. John, O. Breitenstein, and J. Knoch, "Quantitative local current-voltage analysis with different spatially-resolved camera based techniques of silicon solar cells with cracks," in *Proc. IEEE 40th Photovolt. Spec. Conf. (PVSC)*, Jun. 2014, pp. 3473–3478, doi: 10.1109/PVSC.2014.6925680.

[50] S. Rißland and O. Breitenstein, "Considering the distributed series resistance in a two-diode model," *Energy Procedia*, vol. 38, pp. 167–175, Jan. 2013, doi: 10.1016/j.egypro.2013.07.264.

XIAOBO HU received the B.S. degree in physics and the M.S. degree in condensed matter physics from Beijing Normal University, Beijing, China, in 2008 and 2011, respectively, and the Ph.D. degree in applied physics from the University of Tsukuba, Japan, in 2015. He is currently an Associate Professor with East China Normal University, Shanghai, China. His research interest includes characterizations and fabrications of thin-film solar cells.

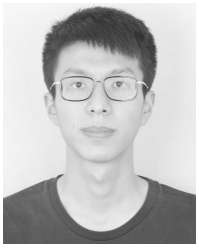

YOUYANG WANG received the B.S. degree from the Department of Electronic Engineering, East China Normal University, Shanghai, China, in 2017, where he is currently pursuing the Ph.D. degree. His current research interests include electrical modeling of photovoltaic devices, III-V compound solar cell diagnosis, and thin-film solar cell characterizations.

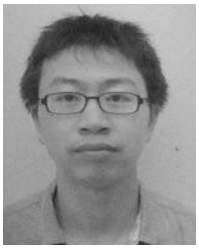

YUN JIA received the B.S. degree from the School of Information Science and Technology, Nantong University, Nantong, China, in 2019. He is currently pursuing the M.S. degree with the Department of Electronic Engineering, East China Normal University, Shanghai, China. His current research interest includes photovoltaic devices modeling, characterizations, and fabrications.

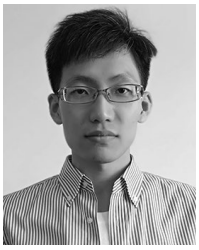

JIANYU HONG received the B.S. degree in microelectronics science and engineering from China Jiliang University, Hangzhou, China, in 2017. He is currently pursuing the M.S. degree with the Department of Electronic Engineering, East China Normal University, Shanghai, China. His current research interests include solar cell modeling and defect diagnosis.

TENGFEI CHEN received the B.S. degree in electrical science and applied physics from the Hefei University of Technology, Hefei, China, in 2015, and the M.S. degree from the Department of Electronic Engineering, East China Normal University, Shanghai, China, in 2018. His research interest includes integrated circuits.

JUANJUAN XUE received the B.S. degree from the Department of Physical Engineering, Zhengzhou University, Zhengzhou, China, in 2015. She is currently pursuing the Ph.D. degree with the Department of Electronic Engineering, East China Normal University, Shanghai, China. Her current research interests include fabrication thin-film solar cell and characterization of defects in thin-film solar cell devices.

YUANJING CHEN received the B.S. degree from the Department of Electronic Engineering, East China Normal University, Shanghai, China, in 2018, where she is currently pursuing the M.S. degree. Her current research interest includes solar cell modeling and fabrications.

JIAHUA TAO received the Ph.D. degree from the Key Laboratory of Polar Materials and Devices, Ministry of Education, Department of Electronic Engineering, East China Normal University, Shanghai, China. From 2011 to 2013, he worked with Mengzi Mining and Metallurgy Company Ltd., Yunnan. He currently works as a Postdoctoral Researcher with the School of Physics and Electronic Science, East China Normal University. He has published over 50 articles. His main research interests include novel materials and Cu_2ZnSnS_4 and Sb_2Se_3 thin-film solar cells.

GUOEN WENG was born in Fujian, China, in 1988. He received the B.S. degree in physics from Yangzhou University, Yangzhou, China, in 2010, and the Ph.D. degree in microelectronics and solid electronics from Xiamen University, Xiamen, China, in 2015. He is currently an Associate Professor with East China Normal University, Shanghai, China. His current research interests include III-nitride semiconductor lasers, vertical-cavity surface-emitting lasers, lead halide-based perovskite materials, and optoelectronic devices.

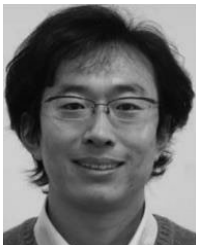

SHAOQIANG CHEN received the B.S. and M.S. degrees in electronic engineering from East China Normal University, Shanghai, China, in 2002 and 2005, respectively, and the Ph.D. degree in applied physics from the University of Tsukuba, Japan, in 2009. He is currently a Professor with East China Normal University. His research interests include semiconductor laser and opto-electrical devices, such as photovoltaic devices and light emitting devices.

ZIQIANG ZHU received the M.S. and Ph.D. degrees in electrical engineering from Shizuoka University, Hamamatsu, Japan, in 1987 and 1990, respectively. From 1994 to 1998, he was a Research Associate with the Institute for Materials Research, Tohoku University, Sendai, Japan. He is currently a Lifetime Professor with East China Normal University, Shanghai, China. He has gained international recognition for research in semiconductor materials and devices, condense physics, IC and MEMS technology, biosensors, and gene chips.

JUNHAO CHU received the Ph.D. degree from the Shanghai Institute of Technical Physics, Chinese Academy of Sciences, in 1984. From 1986 to 1988, he was a Humboldt Fellow with the Technical University of Munich, Germany. He is currently a Faculty Member of the Chinese Academy of Sciences. He is also a Professor with the Shanghai Institute of Technical Physics, Chinese Academy of Sciences. He is also the Director of the Shanghai Center for Photovoltaics. He is also a Professor with East China Normal University. He is a Chinese semiconductor physics and device experts. He has made a systematically investigation on the opto-electronics of narrow gap semiconductors and low dimensional system of semiconductors.